Radar Communication System Recalibration using DNN-based Unscented Kalman Filter Modeling

Williams-Paul Nwadiugwu, , and Dong-Seong Kim,
ICT Convergence Research Center, Dept. of IT Convergence Engineering,
Kumoh National Institute of Technology, Gumi, 39177, South Korea.
{williams.nwa@kumoh.ac.kr; dskim@kumoh.ac.kr}

***Abstract*—In typical air traffic control (ATC) scenario where it is apparently challenging to deploy aircraft for special missions as reconnaissance and surveillance, a proposed ACD-UKF model becomes suitable especially where operational flexibility and without manual aircraft-turning are prioritized objectives. In this paper, novel deep neural network model (DNN) enhanced accurate continuous-discrete unscented Kalman filtering (ACD-UKF) model for a radar's ordinary differential equation (ODE) solver system navigation tool is presented. The ODE solver system essentially works to control radar navigation parameters with-respect-to (w.r.t) global error control, monitoring metrics and tracking capabilities. With the proposed DNN scheme, limitations resulting from matrix factorization are addressed. A seven-dimensional (7-D) radar tracking drawback in constrained condition is mirrored, allowing the deployed aircraft to conduct supervised turns using the proposed ACD-UKF model. Performance evaluation was then conducted where real-time factors such as the system's outage thresholds, network sum-rate and yaw differences for the global navigation satellite system (GNSS) propelled aircraft radar tracker data-set, in stationary and in accelerating positions were trained and validated using the proposed DNN model.**

***Index Terms*—Aircraft turns, DNN-based ACD-UKF, IMU/GNSS, LSTM, ODE, *yaw* differences.**

I. Introduction

The current GNSS-propelled radar technologies [1]-[3], deployed for space-air-ground integrated network (SAGIN) [4] systems have been widely investigated. The use of Kalman filter (KF) models have provided dissimilar and nonlinear results for guaranteeing global error control handling for typical air traffic control systems. Advancements from basic KF to continuous-discrete (CD) KF [5]-[10], (including the cubature, extended and unscented Kalman filter models), presented up-scaled versions for SAGIN-reliant systems. In [5]-[6], accuracy was achieved by using the third-degree spherical-radial cubature rule, meant for Gaussian-weighted integral computations. These computations are derived from nonlinear discrete-time state-space stochastic KF approaches. In [7]-[10], various approaches using the form (1) order were derived and then implemented in diverse research areas.

Recent agile research works have further expanded major existing models and replaced them with more ACD-KF models. These models are essentially derived from the EKF model and are considered to be more robust and suitable for target tracking, in comparison to the earlier models [11]. They are structurally hinged upon a Runge-Kutta pairings. This work capitalizes on the Runge-Kutta based EKF pairing with an unscented part of the Mazzoni's model (M2) [12], hence, forming a hybrid accurate continuous-discrete unscented Kalman filtering (ACD-UKF) computation model. With increased optimality ratios, this model evaluates predicted error covariance matrix. This model has the capacity to deploy predicted state mean with preassigned accuracy for guaranteeing automatic global error control.

Since the existing ACD-UKF model is mainly deployed for discrete stochastic environment [13]-[14], a summary of our contributions in this paper are as follows:

- The existing approach is then extended into a stochastic differential equation (SDE) model, where hybrid models of the popular Runge-Kutta based EKF pairing with unscented part of Mazzoni's model (M2) is designed.
- Enhanced deep neural network (DNN) based long short-term memory (LSTM) architecture is then proposed to determine the time series for the ACD-UKF model action.
- The outage thresholds, network sum-rate and *yaw* differences for the GNSS-based aircraft radar tracker in stationary and in accelerating positions were further analyzed.

The rest of this paper is structured as follows. The design analysis, detailing inherent radar tracking problems is discussed in section II. The proposed ACD-UKF model for aircraft-turn-coordinated radar tracking is investigated in section III. The system's results and performance evaluation is presented in section IV, while section V concludes this work.

II. Problem Formulation

A. *Aircraft-Turn-Coordinated Radar Tracking Problem*

In typical aircraft trajectory dynamics, where a coordinated turn in horizontal plane is commonly applicable, the stochastic differential equation (SDE) rules are observed. The SDE rule introduces a state vector which is deduced as follows:

$$X(t) := [x(t), \dot{x}(t), y(t), \dot{y}(t), z(t), \dot{z}(t), \omega(t)]^T \in R^{(7)} \quad (1)$$

where x(t), y(t), z(t), and $\dot{x}(t)$, $\dot{y}(t)$, $\dot{z}(t)$ denotes its respective positions with corresponding velocities in the Cartesian coordinates of time *t*. The almost constant turn rate is $\omega(t)$. From the above vector illustration, the system's drift rate can now be deduced as:

$$F(.) := [\dot{x}(t), -\omega(t)\dot{y}(t), \dot{y}(t), \omega(t)\dot{x}(t), \dot{z}(t), 0, 0]^T \in R^{(7)} \quad (2)$$

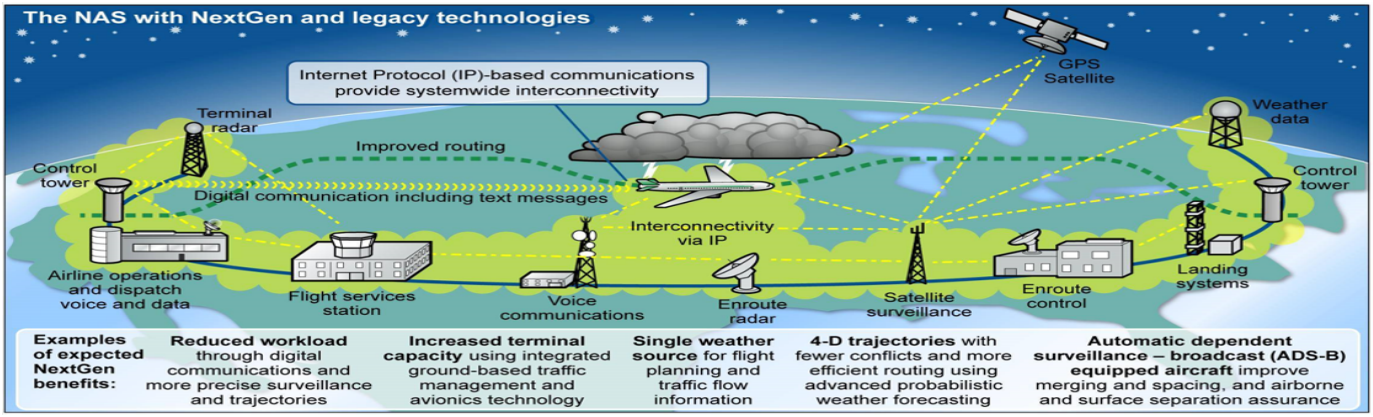

Fig. 1. A typical aircraft-based radar-to-air traffic control system architecture. The architecture depicts the three-way communication environment that exists among the aircraft, the ATC and the radar/communication satellite.

where the stochastic noise term is 7-D with sequential entries as: $\{\omega_i(t),\ t \geq 0\}$, i = 1,..., 7. The entries are mutually independent Brownian processes which are properly channeled into the SDE process. This is important since unpredictable errors resulting from turbulence and other climatic factors are to be mirrored, leading to the derivation of diagonal matrix G:

$$G := diag[0, \sigma_1, 0, \sigma_1, 0, \sigma_1, \sigma_2] \tag{3}$$

with limits of $\sigma_1 = \sqrt{0.20}$, and limits of $\sigma_1 = \sqrt{0.007}$.

B. Air Traffic Control Case-Study

In this part, air traffic control scenario measurement equation is depicted in nonlinear and discrete-time graph. These core graphs are addressed using its measurement vector as:

$$Z_k := [r_k, \theta_k, \phi_k]^T \in R^{(3)} \tag{4}$$

and its measurement function:

$$h(.) := \begin{bmatrix} \sqrt{x_k^2 + y_k^2 + z_k^2} \\ tan^{-1}(y_k/x_k) \\ tan^{-1}(z_k/\sqrt{x_k^2 + y_k^2}) \end{bmatrix} \in R^{(3)}. \tag{5}$$

where the coordinates x_k, y_k, z_k are the aircraft's position in a time t_k. These measurement equations is mirrored with the radar position, equipped with range *r*, azimuth angle θ and elevation angle ϕ, all at its origin. Therefore, a computation of the measurement noise becomes $v_k \approx N(0, R)$, where R := $diag[\sigma_r^2, \sigma_\theta^2, \sigma_\phi^2]$ and $\sigma_r = 50$, $\sigma_\theta = 0.1°$, and $\sigma_\phi = 0.1°$. The illustrated air traffic case study is numerically processed in time lapse $0\ s \leq 210\ s$, while the aircraft's initial state is pre-determined using the vector parameters deduced as:

$$\bar{X} := [1000m, 0m/s, 2650m, 150m/s, 200m, 0m/s\omega°/s]^T \tag{6}$$

where ω = 3,4.5,6. Then the initial covariance is taken to be

$$\prod_0 := [0.01, 0.01, 0.01, 0.01, 0.01, 0.01, 0.01]. \tag{7}$$

The model is adjudged to higher optimality ratios, in comparison to all other exiting models. this was strongly corroborated owing to its robustness (hybridized model) and the ability to allow for multiple and dissimilar number of SDE data samplings. The system's block diagram is illustrated in Fig. 1.

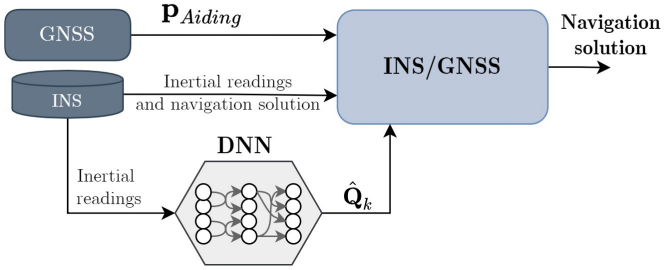

Fig. 2. Proposed system model with block diagrams showing the proposed deployment of ACD-UKF model. The aircraft-turn-coordinated radar system is embedded with the proposed ACD-UKF to manipulate the initial data samplings from the air traffic control center. Our adaptive hybrid adaptive filter applied to the INS/GNSS fusion process to tune the process noise covariance matrix, . Both IMU and GNSS measurements are plugged into the INS/GNSS filter, while the six IMU channels are also inserted into the DNN for predicting the process noise covariance matrix.

III. Proposed ACD-UKF Model

A re-calibration of the radar communication system protocol is proposed. To achieve this, ACD-UKF model [15] is derived by obtaining the discretized continuous-time system process. The values obtained are then channeled into the additive zero-mean noise case UKF as obtained in [16, Appendix B], to successfully build (i) a novel square root model for ACD-UKF version in Algorithm 1 to determine both the system's execution time and measurement updates in Algorithm 2. The system's (ii) parameter sub-vector and (iii) cross-covariance matrix are further determined and obtained. Block diagrams of the proposed ACD-UKF model as deployed in this work are captured in Fig. 2. This is capitulated in the step-wise m-step ACD-UKF approach.

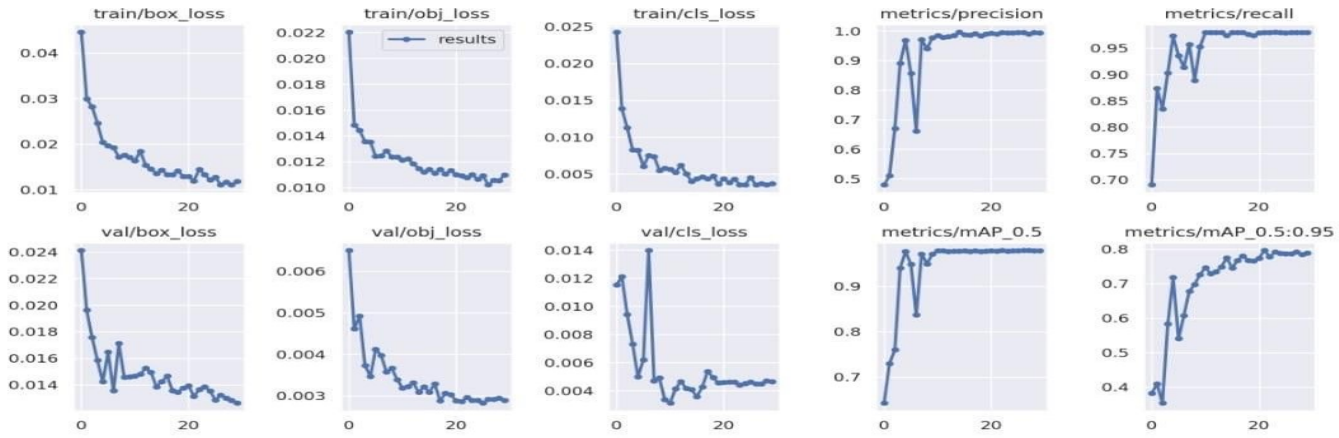

Fig. 3. *Yaw* differences for drones in constant velocity and averaging total of 20 filter runs where loss decrement w.r.t number of epochs and metrics increment w.r.t number of epochs are depicted.

Algorithm 1: Time update in ACD-UKF modeling.

Start: Initial covariance square root $\prod_0^{1/2}$ is derived.
Setting: $P_{0|0}^{1/2} := \prod_0^{1/2}$, $\hat{x}_{0|0} := \bar{x}_0$, $\epsilon_g := 10^{-4}$.
Looping: For K := 1,2,...,K (where K is sampling instants for SDE model (1) interval simulations).
Time update: Given that $\hat{x}_{k-1|k-1}$ and $P_{k-1|k-1}^{1/2}$, compute predicted covariance matrix square root $P_{k-1|k-1}^{1/2}$, and predicted state mean $\hat{x}_{k-1|k-1}$.
for $\epsilon_{loc} := \epsilon_{loc}^{3/2}$, τ_{max} := *0.1, M := 1,* **do**

ℓ:=0, M:=0, τ_0:=min{0.01, δ}, $P_0^{1/2}$:=$P_{k-1|k-1}^{1/2}$, $\hat{x}_{k-1|k-1}^4$, $\Delta\hat{x}_0$:=0, $|\Delta\hat{x}|_{max}$:=0, t_0:=t_{k-1};
While ($t_\ell < t_k$) & ($|\Delta\hat{x}\ell|_{sc} \leq 10\epsilon_g$) **do**;
$t_{\ell+1} := t_\ell + \tau_\ell$, compute $\hat{x}_{\ell+1}^4$, $\hat{x}_{\ell 2}^{2,4}$ in (8) and the scaled error local error $|\ell e_{\ell+1}|_{sc}$ in (9) and (10);
$\tau_\ell^* := \min\{1.5, 0.8(\epsilon_{loc}/|\ell e_{\ell+1}|_{sc})^{1/3}\}\tau_\ell$;
If $|\ell e_{\ell+1}|_{sc} \geq \epsilon_g$, **then** $\tau_\ell := \tau_\ell^*$; **else do;**
Evaluate the error $|\Delta\hat{x}_{\ell+1}|_{sc}$ in (11) and (12);
$|\Delta\hat{x}|_{max} := \max\{|\Delta\hat{x}|_{max}, |\Delta\hat{x}_{\ell+1}|_{sc}\}$;
If $|\Delta\hat{x}_{\ell+1}|_{sc} \gg \epsilon_g$, **then** M := 1;
If M = 0, **then do**;
The Cholesky decomposition equation is applied, where: $Q_{\ell+1/2} = Q_{\ell+1/2}^{1/2} * Q_{\ell+1/2}^{T/2}$;
Compute $P_{\ell+1}^{1/2}$ in (14),(15); end{then};
$\tau_{\ell+1} := \min\{\tau_\ell^*, t_k - t_{\ell+1}, \tau_{max}\}$;
$\ell := \ell + 1$;
End{else};
End{while};
If M = 1, then $\epsilon_{loc} := (0.8\epsilon_g/|\Delta\hat{x}|_{max})^{3/2}\epsilon_{loc}$;
End{while};
Stop

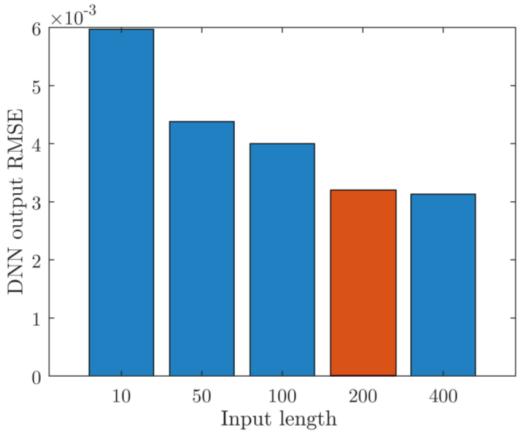

Fig. 4. The RMSE variations of the proposed deep neural network (DNN) versus the input length (N)

A. *DNN-based ACD-UKF Square-root Filtered Algorithms*

The popular recurrent DNN approach is investigated. In particular, the long short-term memory (LSTM) architecture to determine the time series data in Algorithm 1 is deployed. During the training phase the DNN learns the optimal weights of the kernels. The GNSS position updates are employed to aid the INS [17] and demonstrate our hybrid learning approach. Applying the suggested adaptive tuning approach in online setting involves integrating the INS/GNSS with the regressor as depicted in Fig. 2. The numerical outcome in this section buttressed the solution vector $\hat{x}_L^4$ and matrix $P_L^{1/2}$ the subscript L marks the last node in the generated mesh $\{t_\ell\}$ (i.e., tL $\equiv$ tk), are taken as the output of our proposed ACD-UKF solver applied to MDEs (2), (3) for calculating the predicted state expectation and the predicted covariance matrix square root with the scaled global error not exceeding ϵ_g. Extension of these limitation is observed in the proposed tightly-fixed GPS/IMU-enabled drones, where negligibility of cross covariance matrix causes smaller Kalman

Algorithm 2: Measurement update in ACD-UKF

Start: Predicted state mean $\hat{x}_{k|k-1}$ and predicted covariance square root $P^{1/2}_{k|k-1}$ are obtained.

Setting: $P^{1/2}_{0|0} := \prod^{1/2}_0$, $\hat{x}_{0|0} := \bar{x}_0$, $\epsilon_g := 10^{-4}$.

Looping: For when sets of 2_n cubature nodes ξ_i are to be created.

Measurement update: Given that $\hat{x}_{k|k-1}$ and $P^{1/2}_{k|k-1}$, compute predicted covariance matrix square root $P^{1/2}_{k|k-1}$, and predicted state mean $\hat{x}_{k-1|k-1}$.

For when sets of 2n cubature nodes ξ_i are created.

$$\xi_i := \begin{cases} \sqrt{ne_\ell} & \text{where} \quad i = 1, ..., n, \\ \sqrt[1]{ne_{\ell-n}} & \text{where} \quad i = n+1, ..., 2n \end{cases}$$

The aircraft's sub-vectors are then determined as:

$\varsigma_{i,k|k} := \hat{x}_{i,k|k} + P^{1/2}_{k|k-1}\xi_i, i = n+1, ..., 2n.$

Sub-vector (1) is transformed with the function *h(.)* as:

$\eta_{i,k|k} := h(\varsigma_{i,k|k}), i = n+1, ..., 2n$

The predicted measurement update is then estimated using: $\hat{z}_{i,k|k} := \frac{1}{2n}\sum^{2n}_{i=1}\eta_{i,k|k}$

To obtain the measurement noise covariance square root $R^{1/2}_k$, the Cholesky decomposition equation is applied, where: $R_k = R^{1/2}_k * R^T_k$;

Further compute the followings:

Covariance matrix $\bar{P}_{xz,k}$, Innovations covariance square root $R^{1/2}_{e,k}$, and Filtering covariance matrix square root $P^{1/2}_{k|k}$, thus:

$$\begin{bmatrix} \chi_{k|k-1} & R^{1/2}_k \\ Z_{k|k-1} & 0 \end{bmatrix} * \Theta_k = \begin{bmatrix} R^{1/2}_{e,k} & 0 \\ \bar{P}_{xz,k} & P^{1/2}_{k|k} \end{bmatrix}.$$

where weighted-centered matrices of size n × 2n are:

$\chi_{k|k-1} = \frac{1}{\sqrt{2n}} * [\varsigma_{1,k|k-1} - \hat{x}_{k|k-1}, ..., \varsigma_{2n,k|k-1} - \hat{x}_{k|k-1}].$

$Z_{k|k-1} = \frac{1}{\sqrt{2n}} * [\eta_{1,k|k-1} - \hat{z}_{k|k-1}, ..., \eta_{2n,k|k-1} - \hat{z}_{k|k-1}].$

Then proceed to determine the Continuous-discreet cubature gain matrix $W_k = \bar{P}_{xz,k} * R^{-1/2}_{e,k}$.

Conclusively, the filtering state mean $\hat{}_{k|k}$ is determined at the next sampling time t_k using the equation: $\hat{x}_{k|k} = \hat{x}_{k|k-1} + W_k(z_k - \hat{z}_{k|k-1})$.

Stop

gain thereby, limiting convergence speed. The flexibility of this approach at adopting different state's estimation for the two introduced sub-vectors implies its capability at multi-updating, guaranteeing estimation accuracy and further ensuring that the computational loads are kept at barest minimum.

IV. Performance Evaluation and Discussion

The deployed DNN based ACD-UKF model was trained using datasets obtained in Section III-A. After atleast 20 to 30 epochs, the system achieved an root-mean-square-error (RMSE) value of between 0.04 for the train and 1.0 for the metrics. Output results in Fig. 3 illustrates the loss decrement versus the number of epochs and the metrics increment versus number of epochs. The result stipulates that with faster and higher metrics of 0.04 or above, while keeping losses at barest minimal 20.0 or below, the better will be the system model. This improvement also demonstrates the robustness and generalization properties of the proposed DNN architecture, enabling it to cope with unseen data from different IMU sensors. In addition, and together with the trained data-set results, it proves our hypothesis of regressing only the first six elements in the diagonal of the continuous process noise covariance. Although demonstrated for quadrotor INS GNSS fusion, the proposed approach can be elaborated for any external sensor aiding the INS and for any type of platform.

TABLE I
Simulation Parameters

Parameter	Values
Drone transmitting power	30 dBm
Drone noise power σ	-80 dBm
Path-loss exponent α	3
Rician factor *K*	0, 5, 10 dB
SNR threshold ϑ	0, 5, 10 dB
Frequency range	$\leq$ 30 KHz
Sound's speed range	1500m/s
Coverage area	1250 m
Propagated energy	0.5 Watt

In Fig. 4, result show that the INS/GNSS fusion is mostly performed under realtime conditions, where latency in the position computation might degrade the performance. Thus, the influence of the IMU sequence length input was examined. The system noise covariance matrix was learned, based on series of length N. As N ¿¿ 1, the probability of learning the correct terms grows, since the DNN can capture the signal intrinsic properties easier using more data; however, the latency grows. Considering this trade-off, we trained the chosen architecture with various N values and calculated the root-mean-square-error (RMSE) as shown in Fig. 4. As expected, N = 400 obtained the minimum RMSE, yet for the rest of the analysis we chose N = 200 (similar RMSE) to receive the regression result as it is given in a shorter time period. For example, in the stimulative train and test dataset the sampling rate is 100Hz, thus working with N = 200 gives the regression result every two seconds instead of working with four seconds (N = 400).

V. Conclusion

A seven-dimensional (7-D) radar tracking drawback in critical environmental condition is examined, allowing the deployed aircraft to conduct supervised turns using the proposed ACD-UKF model. Since it is challenging to deploy aircraft for such purpose, novel ACD-UKF model was promoted. The proposed ACD-UKF becomes suitable and possessing key beneficial features such as operational flexibility, without manual aircraft-turning for typical ATC scenario. Other key inherent ACD-UKF features as demonstrated are its ability

at conducting and successfully processing dissimilar radar-to-ATC initial data sampling, and doing so in multiple time-lapses. As part of our future works, we intend to capitalize on the existing model to harness more energy-reliant scheme.

VI. Acknowledgment

This research is supported by Priority Research Centers Program through NRF funded by MEST (2018R1A6A1A03024003), and Grand ICT Research Center support program of MSIT (IITP-2020-2020-0-01612), South Korea.

References

[1] M.A. Rabbou and A. El-Rabbany, "Tightly coupled integration of GPS precise point positioning and MEMS-based inertial systems," *GPS Solutions*, pp. 601-609, 2015, https://doi.org/10.1007/s10291-014-0415-3.

[2] M. Coutino, E. Isufi, T. Maehara and G. Leus, "State-Space Network Topology Identification From Partial Observations," *IEEE Transactions on Signal and Information Processing over Networks,* vol. 6, pp. 211-225, 2020, doi: 10.1109/TSIPN.2020.2975393.

[3] Y. -C. Lai and T. -Q. Le, "Adaptive Learning-Based Observer With Dynamic Inversion for the Autonomous Flight of an Unmanned Helicopter," *IEEE Transactions on Aerospace and Electronic Systems,* vol. 57, no. 3, pp. 1803-1814, June 2021, doi: 10.1109/TAES.2021.3050653.

[4] W. Nwadiugwu and D. Kim, "Ultrawideband Network Channel Models for Next-Generation Wireless Avionic System," *IEEE Transactions on Aerospace and Electronic Systems*, vol. 56, no. 1, pp. 113-129, Feb. 2020.

[5] G. Y. Kulikov and M. V. Kulikova, "Accurate State Estimation in Continuous-Discrete Stochastic State-Space Systems With Nonlinear or Nondifferentiable Observations," *IEEE Transactions on Automatic Control,* vol. 62, no. 8, pp. 4243-4250, Aug. 2017.

[6] G. Y. Kulikov and M. V. Kulikova, "The Accurate Continuous-Discrete Extended Kalman Filter for Radar Tracking," *IEEE Transactions on Signal Processing,* vol. 64, no. 4, pp. 948-958, Feb.15, 2016.

[7] M. V. Kulikova, "Square-Root Approach for Chandrasekhar-Based Maximum Correntropy Kalman Filtering," *IEEE Signal Processing Letters,* vol. 26, no. 12, pp. 1803-1807, Dec. 2019.

[8] J. V. Tsyganova and M. V. Kulikova, "SVD-Based Kalman Filter Derivative Computation," *IEEE Transactions on Automatic Control,* vol. 62, no. 9, pp. 4869-4875, Sept. 2017, doi: 10.1109/TAC.2017.2694350.

[9] T. Vercauteren and Xiaodong Wang, "Decentralized sigma-point information filters for target tracking in collaborative sensor networks," *IEEE Transactions on Signal Processing,* vol. 53, no. 8, pp. 2997-3009, 2005.

[10] M. Zhu, W. Ouyang and Y. Wu, "Orientation Estimation by Partial-State Updating Kalman Filter and Vectorial Magnetic Interference Detection," *IEEE Transactions on Aerospace and Electronic Systems,* doi: 10.1109/TAES.2021.3050657.

[11] M. S. Grewal, L. R.Weill, and A. P. Andrews, " Global Positioning Syst., Inertial Navigat. & Integration." *New York, NY, USA:Wiley,* 2001.

[12] S. Sarkka, "On Unscented Kalman Filtering for State Estimation of Continuous-Time Nonlinear Systems," *IEEE Transactions on Automatic Control,* vol. 52, no. 9, pp. 1631-1641, Sept. 2007.

[13] A. H. Jazwinski, "Stochastic Processes and Filtering Theory." *New York, NY, USA: Academic,* 1970.

[14] B. Øksendal, "Stochastic Differential Equations: An Introduction with Applications." *New York, NY, USA: Springer,* 2003.

[15] W. -P. Nwadiugwu, S. -H. Kim and D. -S. Kim, "Precise-Point-Positioning Estimations for Recreational Drones Using Optimized Cubature-Extended Kalman Filtering," *IEEE Access,* vol. 9, pp. 134369-134383, 2021, doi: 10.1109/ACCESS.2021.3116058.

[16] I. Arasaratnam, S. Haykin and T. R. Hurd, "Cubature Kalman Filtering for Continuous-Discrete Systems: Theory and Simulations," *IEEE Transactions on Signal Processing,* vol. 58, no. 10, pp. 4977-4993, Oct. 2010.

[17] P. D. Groves, "Principles of gnss, inertial, and multisensor integrated navigation systems, [book review]," *IEEE Aerospace and Electronic Systems Magazine,* vol. 30, no. 2, pp. 26–27, 2015.